Hydrogenases

International Edition: DOI: 10.1002/anie.201805144
German Edition: DOI: 10.1002/ange.201805144

Terminal Hydride Species in [FeFe]-Hydrogenases Are Vibrationally Coupled to the Active Site Environment

Cindy C. Pham[+], David W. Mulder[+], Vladimir Pelmenschikov[+], Paul W. King, Michael W. Ratzloff, Hongxin Wang, Nakul Mishra, Esen E. Alp, Jiyong Zhao, Michael Y. Hu, Kenji Tamasaku, Yoshitaka Yoda, and Stephen P. Cramer**

Abstract: *A combination of nuclear resonance vibrational spectroscopy (NRVS), FTIR spectroscopy, and DFT calculations was used to observe and characterize Fe–H/D bending modes in CrHydA1 [FeFe]-hydrogenase Cys-to-Ser variant C169S. Mutagenesis of cysteine to serine at position 169 changes the functional group adjacent to the H-cluster from a -SH to -OH, thus altering the proton transfer pathway. The catalytic activity of C169S is significantly reduced compared to that of native CrHydA1, presumably owing to less efficient proton transfer to the H-cluster. This mutation enabled effective capture of a hydride/deuteride intermediate and facilitated direct detection of the Fe–H/D normal modes. We observed a significant shift to higher frequency in an Fe–H bending mode of the C169S variant, as compared to previous findings with reconstituted native and oxadithiolate (ODT)-substituted CrHydA1. On the basis of DFT calculations, we propose that this shift is caused by the stronger interaction of the -OH group of C169S with the bridgehead -NH- moiety of the active site, as compared to that of the -SH group of C169 in the native enzyme.*

Hydrogenases (H_2ases) are enzymes that catalyze the reversible interconversion of molecular hydrogen into protons and electrons: $H_2 \rightleftarrows 2H^+ + 2e^-$.[1] Under optimal electron delivery, H_2ases require little or no driving force while utilizing base transition metals as catalytic cofactors. The [FeFe]-H_2ases are known to display exceptionally high turnover rates of $>10^4\ s^{-1}$.[1a,2] Resolving the mechanistic properties of [FeFe]-H_2ases requires identification of the catalytically relevant intermediates,[3] and is of interest to advancing catalyst design for developing H_2 fuel cells and renewable energy production technologies.[4]

The active site for all known [FeFe]-H_2ases consists of an "H-cluster" that is composed of $[4Fe\text{-}4S]_H$ and $[2Fe]_H$ subclusters, linked by a cysteine thiolate (Figure 1).[6] The main site of catalytic H_2 bond activation is the Fe_d iron site of $[2Fe]_H$ distal to $[4Fe\text{-}4S]_H$, where the azadithiolate (ADT) group plays a fundamental role in proton transfer. The nitrogen N_{ADT} of the ADT bridge is involved in transporting solvent protons to and from Fe_d through a relay of conserved amino acids that lead to the surface of the protein.[7] In one of the simplest structural forms of the enzyme, *Chlamydomonas reinhardtii* [FeFe]-H_2ase HydA1 (*Cr*HydA1), the conserved relay is composed of residues C169, E141, S189, and E144 (Figure 1). The C169 side chain plays a crucial role in catalysis as the -SH group is positioned within hydrogen-bonding distance (ca. 2 Å) to the bridgehead amine of ADT.[7b]

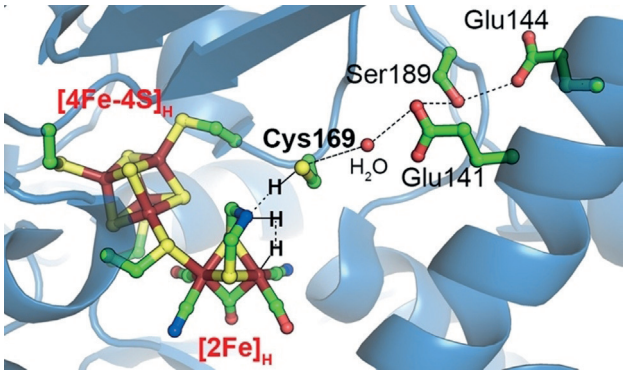

Figure 1. Structural representation of the primary proton transport chain and H_2 bond activation at the H-cluster of [FeFe]-H_2ase. The ADT ligand and C169 residue link proton transfer events to terminal hydride formation at $[2Fe]_H$ through an extended hydrogen-bonding network (dotted lines) composed of several conserved amino acids; the crystal structure from PDB 3C8Y[5] was used for this illustration, and the amino acid numbering is from the *Cr*HydA1 primary sequence. Protonation sites (-H) on $[2Fe]_H$ and C169 of the H_{hyd} state are shown.

Alteration of the ADT bridge or critical amino acids along the proton transfer pathway can abolish or severely reduce the H_2 reduction activity. Examples include the [FeFe]-H_2ase variants C169A and C169S of *Cr*HydA1,[3b,e] C299S of *Clostridium pasteurianum* (*Cp*I), C298S of *Clostridium ace-*

[*] Dr. C. C. Pham,[+] Dr. H. Wang, N. Mishra, Prof. S. P. Cramer
Department of Chemistry, UC Davis
One Shields Ave, Davis, CA 95616 (USA)
E-mail: spjcramer@ucdavis.edu
Dr. D. W. Mulder,[+] Dr. P. W. King, Dr. M. W. Ratzloff
National Renewable Energy Laboratory
15013 Denver W. Pkwy., Golden, CO 80401 (USA)
Dr. V. Pelmenschikov[+]
Institut für Chemie, Technische Universität Berlin
Straße des 17. Juni 135, 10623 Berlin (Germany)
E-mail: pelmentschikov@tu-berlin.de
Dr. E. E. Alp, Dr. J. Zhao, Dr. M. Y. Hu
Building 401, Argonne National Laboratory
9700 Cass Ave, Lemont, IL 60439 (USA)
Dr. K. Tamasaku, Dr. Y. Yoda
JASRI, SPring-8
1-1-1 Kouto, Mizauki-cho, Sayo-gun, Hyogo 679-5198 (Japan)
[+] These authors contributed equally to this work.
Supporting information and the ORCID identification number(s) for the author(s) of this article can be found under: https://doi.org/10.1002/anie.201805144.

tobutylicum (*Ca*HydA), and C178A of *Desulfovibrio desulfuricans* (*Dd*HydAB).[7b,8] Furthermore, by using these modified proteins, one can accumulate significant amounts of an intermediate known as H_{hyd}, which contains a trapped terminal hydride Fe_d–H (Figure 1), and features a $[4Fe\text{-}4S]_H^+$-$Fe_p^{II}Fe_d^{II}$ oxidation state of the H-cluster.[3b,c,e,9]

Nuclear resonance vibrational spectroscopy (NRVS), also known as nuclear inelastic scattering (NIS), is a synchrotron-based X-ray technique that probes vibrational modes using nuclear excitation in Mössbauer-active isotopes.[10] When applied to ^{57}Fe-labeled proteins, it selectively probes the vibrational motion of ^{57}Fe nuclei. In previous works on *Cr*HydA1 and *Dd*HydAB [FeFe]-H_2ases,[3c,9] we have shown that $^{57}Fe_d$–H bending modes can be observed by NRVS. The NRVS signature of the terminal Fe_d–H hydride in H_{hyd} contains two bands $>670\ cm^{-1}$, which were rationalized by density functional theory (DFT) as H^- hydride motions perpendicular to and within the approximate mirror symmetry plane of $[2Fe]_H$.

Herein, we extend our method to identify the Fe_d-H/D modes in the C169S *Cr*HydA1 variant. Specifically, we report the H_{hyd} ^{57}Fe NRVS spectra of the biosynthesized $[4^{57}Fe\text{-}4S]_H$-$[2^{57}Fe]_H$ C169S *Cr*HydA1 (†C169S) species. We compare this new data to previously reported H_{hyd} spectra for reconstituted $[2^{57}Fe]_H$ native[9] (†RN) and $[2^{57}Fe\text{-ODT}]_H$ bridgehead-altered[3c] (†ODT) enzymes. The NRVS data reveal surprising spectral shifts produced by the -SH (†RN) to -OH (†C169S) substitution in the side-chain functional group. The results are interpreted by DFT modeling of the H-cluster and its environment.

NRVS spectra for the †C169S samples prepared under reducing conditions for H_{hyd} enrichment (documented by FTIR in the Supporting Information, Figure S1) in either H_2O ($^{\dagger}C169S_H$) or D_2O ($^{\dagger}C169S_D$) buffer are illustrated in Figures 2 and S2. Features in the 200–400 cm^{-1} range are primarily due to Fe–S motion, and hence they show little change between H and D isotopologues (Figure 2, top). A benefit from having an ^{57}Fe-enriched $[4^{57}Fe\text{-}4S]_H$ subcluster is the presence of redox-sensitive [4Fe-4S]-specific bands in the NRVS data.[12] As illustrated in Figure 2, the positions of the Fe–S stretching bands at 268 and 362 cm^{-1} align nicely with a previously recorded spectrum of the D14C variant of *Pyrococcus furiosus* (*Pf*) ferredoxin (Fd) in its reduced $[4Fe\text{-}4S]^+$ form.[11] This is consistent with the assignment of H_{hyd} to the $[4Fe\text{-}4S]_H^+$-$Fe_p^{II}Fe_d^{II}$ state, having a reduced, paramagnetic Fe-S cubane.[3b,e] The NRVS features in the 400–600 cm^{-1} range, with weaker intensities and higher vibrational energies than the Fe–S bands, are mostly from modes with Fe–CN/CO character, as reported previously.[13]

At still higher energies, there are bands at 673 (A′) and 772 cm^{-1} (A″), which have been assigned to the Fe_d–H bending modes in the H_{hyd} state (Figure 2, bottom).[3c,9] DFT modeling reveals that these modes contain only about 8% ^{57}Fe and as much as approximately 60–80% H^- contributions to their vibrational energies (see the animations for the key normal modes in the Supporting Information). The A′ and A″ features are red-shifted under D_2O conditions, and an Fe_d–D band (B) appears at 630 cm^{-1}, with its intensity enhanced through coupling to the Fe–CO/CN motions. Band B is thus

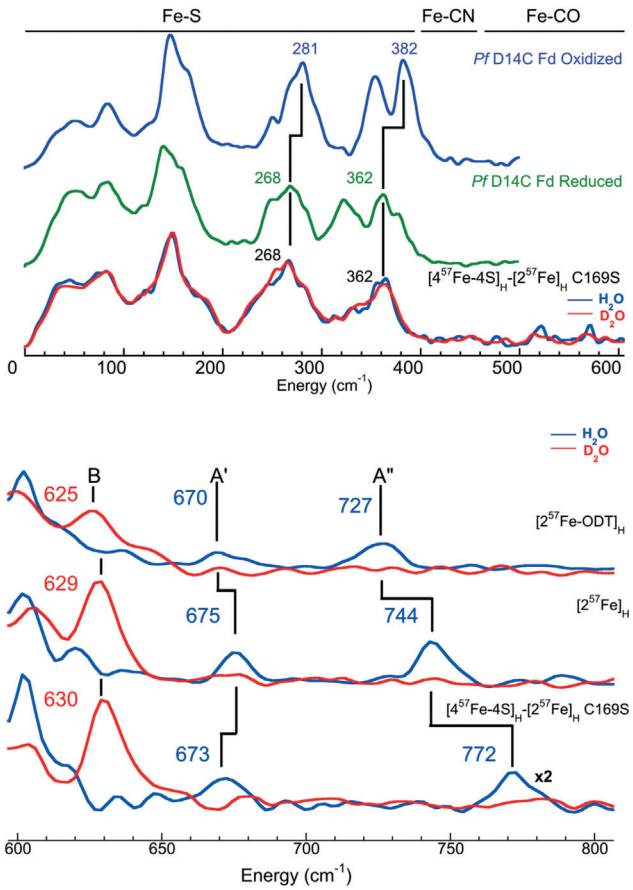

Figure 2. Top: NRVS for H_2O and D_2O samples of $[4^{57}Fe\text{-}4S]_H$-$[2^{57}Fe]_H$ C169S *Cr*HydA1 (†C169S) reduced with sodium dithionite (bottom), compared to the oxidized (top) and reduced (middle) $[4^{57}Fe\text{-}4S]$ cluster from D14C *Pf* Fd.[11] Bottom: Comparison of the Fe_d–H/D bending region recorded using the $[2^{57}Fe\text{-ODT}]_H$ (†ODT),[3c] $[2^{57}Fe]_H$ (†RN),[9] and †C169S samples. Bands A′, A″ and B (see text) are marked.

the most direct evidence for identifying an isotope effect on the Fe_d–H/D modes. The position of band B for the $^{\dagger}C169S_D$ sample insignificantly differs from the previously published NRVS data on bands B from samples $^{\dagger}RN_D$ and $^{\dagger}ODT_D$. The relative positions of bands A′ and A″ of $^{\dagger}ODT_H$, $^{\dagger}RN_H$, and $^{\dagger}C169S_H$ show very different behavior (see also Table S1). Band A′ of $^{\dagger}C169S_H$, compared with $^{\dagger}ODT_H$ and $^{\dagger}RN_H$, undergoes only small shifts within 5 cm^{-1} (Figure 2, bottom), which is below the 8 cm^{-1} instrument resolution of our spectra. However, band A″ of $^{\dagger}C169S_H$ shows a dramatic 28 cm^{-1} upshift relative to $^{\dagger}RN_H$, and an even larger 45 cm^{-1} upshift relative to $^{\dagger}ODT_H$.

As the NRVS spectra for the H_{hyd} state accumulated in the three *Cr*HydA1 samples exhibit prominent shifts in their Fe_d–H bands, a computational model explaining these differences has to include the sample-specific structural variations. Recently, we proposed three levels of DFT modeling for the H-cluster in its H_{hyd} state: *S*, *L*, and *L*′.[9] *S* is a small model that contains the $[2Fe]_H$ subcluster only, which is sufficient to rationalize the variation between the $^{\dagger}ODT_H$ and $^{\dagger}RN_H$ spectra. *L* and *L*′ are larger models, both incorporating as well the $[2Fe]_H$-surrounding amino acids, including the one at position 169; *L*′ additionally includes the $[4Fe\text{-}4S]_H$ cluster

(Figures S4–S7). Model *L* is superior in reproducing the NRVS spectra above 400 cm^{-1} containing the Fe_d–H/D bands, and model *L′* is optimal for the spectral simulation below 400 cm^{-1} (Figure S2). In our previous work on the †RN system, the DFT modeling predicted that the Fe_d–H band structure was indicatively sensitive to the redox level of the $[2Fe]_H$ subcluster; the Fe–H vibrations in both [FeFe]-H_2ase and its model system[14] were found to be sensitive to the details of the environment. A model of H_{hyd} having the -NH- amino form with its H_{ADT} in an "axial" position pointing towards the H_h hydride ($H_{hyd\text{-}A}$ as illustrated in Figure 3, top) was found to be the best fit to the observed NRVS spectra.[9]

The DFT modeling further indicates that inclusion of the $N_{ADT}\cdots H_C/H_S$ hydrogen bond between the ADT bridgehead and C/S169 side chain effectively strengthens the $H_h\cdots H_{ADT}$ dihydrogen interaction (Table 1, *S* vs. *L* values) in both the native enzyme and its C169S variant. The $H_h\cdots H_{ADT}$ interaction, absent in the bridgehead-altered ODT (-O-) species, is crucial for H_2 formation from the H_{hyd} state in the proposed [FeFe]-H_2ase mechanism. Interestingly, the C169S variant is predicted to have an approximately 0.1 Å shorter $H_h\cdots H_{ADT}$ distance than the native enzyme (Table 1, *L* values). Moreover, the optimized C169S *L* model has noticeably shorter $N_{ADT}\cdots H_S$ and $N_{ADT}\cdots O_S$ distances, which characterize the hydrogen bonding between ADT and S169. Overall, the delocalized interactions involving Fe_d–$H_h\cdots H_{ADT}$-$N_{ADT}\cdots H_C$/H_S–S_C/O_S have shorter non-covalent bonding (···) distances in C169S than in the native enzyme, and an approximately 0.8 Å contraction of $Fe_d\cdots O_S = 5.64$ Å versus $Fe_d\cdots S_c = 6.24$ Å.

Even though the $Fe_d\cdots S_C/O_S$ distance is >5 Å, DFT was able to predict the effects of the change in functional group on the Fe_d–H_h vibrational modes. Specifically, there is an approximately 20 cm^{-1} calculated upshift of the ^{57}Fe PVDOS band A″, produced by the delocalized "in-plane" normal mode (involving the hydrogen nuclei H_h of the hydride, H_{ADT} of ADT, and $H_{C/S}$ of C/S169) from 749 (C169) to 768 cm^{-1} (C169S; Figures 3, bottom and S3). In contrast, the lower-energy band A′, produced by the localized "out-of-plane" normal mode (which is essentially a pure Fe_d–H_h motion decoupled from other nuclei) is predicted to be twofold less affected by about 10 cm^{-1}, shifting from 665 (C169) to 675 (C169S) cm^{-1}. The calculations therefore match sufficiently well with the shifts observed by NRVS. Notably, the optimized Fe_d-H_h-H_{ADT} angle is about 110° (Figure 3, top); the H_h displacement vector is therefore approximately in line with the $H_h\cdots H_{ADT}$ bonding for vibrational mode A″, and perpendicular to it for mode A′. Notably, the band B position is essentially invariant to the †ODT$_D$/†RN$_D$/†C169S$_D$ system selection, from both the experiment and theory; the Fe_d–D_h normal mode responsible for B is decoupled from both the cofactor bridgehead and the C/S169 side chain.

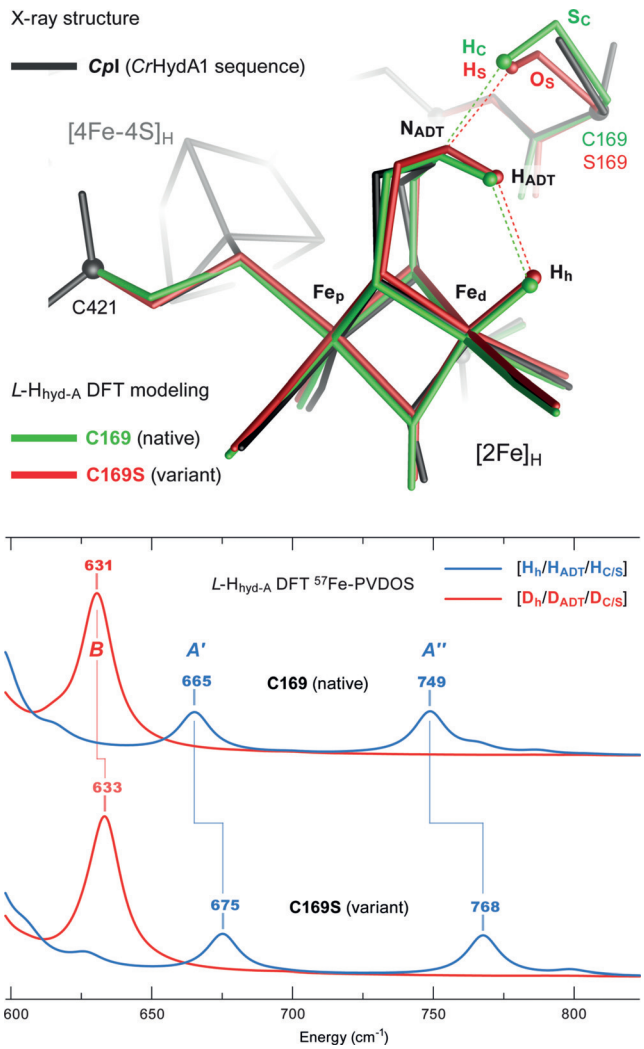

Figure 3. Top: Representative DFT *L* models of the $H_{hyd\text{-}A}$ state in *Cr*HydA1 variants C169 and C169S, overlaid with the X-ray structural reference PDB 5BYQ.[6b] H_h, H_{ADT}, and $H_{C/S}$ sites are shown in ball representation, and other hydrogen nuclei are omitted for clarity. Dashed lines indicate interatomic interactions $H_h\cdots H_{ADT}$ and $N_{ADT}\cdots H_{C/S}$ within 2.3 Å as detailed in Table 1. For the full-size structural view and model alternatives, see Figures S4–S7. Bottom: DFT ^{57}Fe PVDOS spectra >600 cm^{-1} for the †RN and †C169S species based on the best-fit *L*-$H_{hyd\text{-}A}$ modeling. H and D nuclei relevant to the isotope labeling are specified in square brackets. Important bands (A′, A″, and B) associated with the Fe_d–H_h/D_h bending motion are labeled. See Figures S2 and S3 for the 0–900 cm^{-1} spectra, as well as a comparison to the NRVS data.

Table 1: Comparison of key bond lengths and distances in the $H_{hyd\text{-}A}$ state of native C169 and the C169S variant of *Cr*HydA1, optimized at the DFT modeling levels *S* and *L*.

DFT modeling level	Internuclear distance [Å], C169/C169S variant[a]						
	Fe_d–H_h	$H_h\cdots H_{ADT}$	N_{ADT}–H_{ADT}	$N_{ADT}\cdots H_C/H_S$	S_C/O_S–H_C/H_S	$N_{ADT}\cdots S_C/O_S$	$Fe_d\cdots S_C/O_S$
S[b]	1.51	2.14	1.03	NA	NA	NA	NA
L	1.52/1.52	2.01/1.92	1.03/1.03	2.26/ 2.15	1.37/0.98	3.59/3.04	6.24/5.64

[a] Atomic labels follow those used in Figures 3, top and S4–S7. Bonding and non-bonding interactions are indicated in the column headers as "–" and "···", respectively. [b] At the modeling level *S*, the C/S169 residue is not included. The internuclear distances within the $[2Fe]_H$ subcluster therefore take their single values, and "NA" implies distance not applicable.

Implicated in the catalysis, the $H_h\cdots H_{ADT}$ dihydrogen interaction of the H_{hyd} state is therefore stronger in the C169S variant than in the native enzyme. This can be rationalized in terms of the secondary coordination sphere substitution of the more polar -SH thiol group in cysteine ($pK_a \approx 8$) for the less polar -OH hydroxy group in serine ($pK_a \approx 13$), which sets off a cascade of hydrogen-bonding effects linked to the active site. Owing to the large difference in pK_a between the two groups, this structural difference has also been proposed to alter essential proton-transfer steps required for the catalytic mechanism.[8c] The above results indicate that the architecture of the amino acid environment around the H-cluster is critical for attaining an optimal form of the Fe_d–H_h hydride that enables the fast kinetics of the reversible H_2 activation observed in [FeFe]-H_2ases. Analogous model compound studies indeed show that the geometry and precise orientation of the Fe–H Lewis acid–base pair is required to achieve heterolytic H_2 bond cleavage.[15]

Through the combined application of protein mutagenesis, NRVS, FTIR spectroscopy, and DFT calculations, we have elucidated the effects of the modification of the proton transport chain of [FeFe]-H_2ase on its hydride-bound state H_{hyd}. The results reveal that the Cys-to-Ser change modifies structural interactions near the H_2 binding site and the H-cluster ADT ligand. This suggests a broader role for the C169 residue through vibrational coupling in fine-tuning the hydrogen-bonding interactions around the H-cluster required for rapid binding and turnover of H_2. The observation of these effects highlights the potential of NRVS in providing detailed structural information on the [FeFe]-H_2ase active-site environment and, potentially, on other iron-hydride systems. In combination with DFT calculations and site-directed mutagenesis, we have found a synergistic approach to probing the Fe–H vibrational modes and uncovering how they are coupled to the secondary coordination sphere around the active site. We have shown that even an amino acid that is >5 Å away, such as C/S169, modulates the Fe_d–H/D bond in *Cr*HydA1.

Acknowledgements

This work was supported by NIH GM-65440 (S.P.C.) and the Cluster of Excellence EXC 314 "Unifying Concepts in Catalysis" initiative of the DFG (V.P.). This work was authored in part by the Alliance for Sustainable Energy, LLC, the manager and operator of the National Renewable Energy Laboratory for the U.S. Department of Energy (DOE) under Contract No. DE-AC36-08GO28308. Funding for protein purification and FTIR spectroscopy was provided by the U.S. Department of Energy, Office of Basic Energy Sciences, Division of Chemical Sciences, Geosciences, and Biosciences (D.W.M., M.W.R., and P.W.K.). The views expressed in the article do not necessarily represent the views of the DOE or the U.S. Government. The U.S. Government retains and the publisher, by accepting the article for publication, acknowledges that the U.S. Government retains a nonexclusive, paid-up, irrevocable, worldwide license to publish or reproduce the published form of this work, or allow others to do so, for U.S. Government purposes. NRVS experiments were supported by APS (under proposals 44733, 43032, and 49765) and SPring-8 (under JASRI proposals 2015B0103, 2015B1134, 2016A0103, 2016A1154, 2016B1347, 2017A0141, 2017A1115, 2017B0141, 2017B1331 and RIKEN proposals 20150048, 20160063, 20170048.

Conflict of interest

The authors declare no conflict of interest.

Keywords: enzyme catalysis · FTIR spectroscopy · hydride species · hydrogenases · nuclear resonance vibrational spectroscopy

How to cite: *Angew. Chem. Int. Ed.* **2018**, *57*, 10605–10609
Angew. Chem. **2018**, *130*, 10765–10769

[1] a) W. Lubitz, H. Ogata, O. Rudiger, E. Reijerse, *Chem. Rev.* **2014**, *114*, 4081–4148; b) J. W. Peters, G. J. Schut, E. S. Boyd, D. W. Mulder, E. M. Shepard, J. B. Broderick, P. W. King, M. W. W. Adams, *Biochim. Biophys. Acta Mol. Cell Res.* **2015**, *1853*, 1350–1369.

[2] C. Madden, M. D. Vaughn, I. Díez-Pérez, K. A. Brown, P. W. King, D. Gust, A. L. Moore, T. A. Moore, *J. Am. Chem. Soc.* **2012**, *134*, 1577–1582.

[3] a) C. Sommer, A. Adamska-Venkatesh, K. Pawlak, J. A. Birrell, O. Rudiger, E. J. Reijerse, W. Lubitz, *J. Am. Chem. Soc.* **2017**, *139*, 1440–1443; b) D. W. Mulder, Y. Guo, M. W. Ratzloff, P. W. King, *J. Am. Chem. Soc.* **2017**, *139*, 83–86; c) E. J. Reijerse, C. C. Pham, V. Pelmenschikov, R. Gilbert-Wilson, A. Adamska-Venkatesh, J. F. Siebel, L. B. Gee, Y. Yoda, K. Tamasaku, W. Lubitz, T. B. Rauchfuss, S. P. Cramer, *J. Am. Chem. Soc.* **2017**, *139*, 4306–4309; d) M. Winkler, M. Senger, J. F. Duan, J. Esselborn, F. Wittkamp, E. Hofmann, U. P. Apfel, S. T. Stripp, T. Happe, *Nat. Commun.* **2017**, *8*, 0; e) D. W. Mulder, M. W. Ratzloff, M. Bruschi, C. Greco, E. Koonce, J. W. Peters, P. W. King, *J. Am. Chem. Soc.* **2014**, *136*, 15394–15402.

[4] A. De Poulpiquet, A. Ciaccafava, K. Szot, B. Pillain, P. Infossi, M. Guiral, M. Opallo, M. T. Giudici-Orticoni, E. Lojou, *Electroanalysis* **2013**, *25*, 685–695.

[5] A. S. Pandey, T. V. Harris, L. J. Giles, J. W. Peters, R. K. Szilagyi, *J. Am. Chem. Soc.* **2008**, *130*, 4533–4540.

[6] a) G. Berggren, A. Adamska, C. Lambertz, T. R. Simmons, J. Esselborn, M. Atta, S. Gambarelli, J. M. Mouesca, E. Reijerse, W. Lubitz, T. Happe, V. Artero, M. Fontecave, *Nature* **2013**, *499*, 66–69; b) J. Esselborn, N. Muraki, K. Klein, V. Engelbrecht, N. Metzler-Nolte, U.-P. Apfel, E. Hofmann, G. Kurisu, T. Happe, *Chem. Sci.* **2016**, *7*, 959–968.

[7] a) J. C. Fontecilla-Camps, A. Volbeda, C. Cavazza, Y. Nicolet, *Chem. Rev.* **2007**, *107*, 5411–5411; b) A. J. Cornish, K. Gartner, H. Yang, J. W. Peters, E. L. Hegg, *J. Biol. Chem.* **2011**, *286*, 38341–38347; c) J. W. Peters, W. N. Lanzilotta, B. J. Lemon, L. C. Seefeldt, *Science* **1998**, *282*, 1853–1858; d) H. Long, P. W. King, C. H. Chang, *J. Phys. Chem. B* **2014**, *118*, 890–900; e) B. Ginovska-Pangovska, M. H. Ho, J. C. Linehan, Y. H. Cheng, M. Dupuis, S. Raugei, W. J. Shaw, *Biochim. Biophys. Acta Bioenerg.* **2014**, *1837*, 131–138.

[8] a) S. Morra, A. Giraudo, G. Di Nardo, P. W. King, G. Gilardi, F. Valetti, *PLOS One* **2012**, *7*, e48400; b) T. Lautier, P. Ezanno, C. Baffert, V. Fourmond, L. Cournac, J. C. Fontecilla-Camps, P. Soucaille, P. Bertrand, I. Meynial-Salles, C. Leger, *Faraday Discuss.* **2011**, *148*, 385–407; c) P. Knörzer, A. Silakov, C. E.

Foster, F. A. Armstrong, W. Lubitz, T. Happe, *J. Biol. Chem.* **2012**, *287*, 1489 – 1499.
[9] V. Pelmenschikov, J. A. Birrell, C. C. Pham, N. Mishra, H. X. Wang, C. Sommer, E. Reijerse, C. P. Richers, K. Tamasaku, Y. Yoda, T. B. Rauchfuss, W. Lubitz, S. P. Cramer, *J. Am. Chem. Soc.* **2017**, *139*, 16894 – 16902.
[10] a) A. Chumakov, W. Sturhahn, *Hyperfine Interact.* **1999**, *123*, 781 – 808; b) W. Sturhahn, T. S. Toellner, E. E. Alp, X. Zhang, M. Ando, Y. Yoda, S. Kikuta, M. Seto, C. W. Kimball, B. Dabrowski, *Phys. Rev. Lett.* **1995**, *74*, 3832 – 3835.
[11] D. Mitra, V. Pelmenschikov, Y. Guo, D. A. Case, H. Wang, W. Dong, M.-L. Tan, T. Ichiye, J. Francis, E. Jenney, M. W. W. Adams, Y. Yoda, J. Zhao, S. P. Cramer, *Biochemistry* **2011**, *50*, 5220 – 5235.
[12] a) A. Adamska-Venkatesh, T. R. Simmons, J. F. Siebel, V. Artero, M. Fontecave, E. Reijerse, W. Lubitz, *Phys. Chem. Chem. Phys.* **2015**, *17*, 5421 – 5430; b) J. Esselborn, C. Lambertz, A. Adamska-Venkatesh, T. Simmons, G. Berggren, J. Nothl, J. Siebel, A. Hemschemeier, V. Artero, E. Reijerse, M. Fontecave, W. Lubitz, T. Happe, *Nat. Chem. Biol.* **2013**, *9*, 607 – 609; c) B. E. Barton, M. T. Olsen, T. B. Rauchfuss, *Curr. Opin. Biotechnol.* **2010**, *21*, 292 – 297.
[13] a) R. Gilbert-Wilson, J. F. Siebel, C. C. Pham, A. Adamska-Venkatesh, E. Reijerse, H. Wang, S. P. Cramer, W. Lubitz, T. B. Rauchfuss, *J. Am. Chem. Soc.* **2015**, *137*, 8998 – 9005; b) A. M. Lunsford, C. C. Beto, S. D. Ding, O. F. Erdem, N. Wang, N. Bhuvanesh, M. B. Hall, M. Y. Darensbourg, *Chem. Sci.* **2016**, *7*, 3710 – 3719.
[14] M. R. Carlson, D. L. Gray, C. P. Richers, W. Wang, P. H. Zhao, T. B. Rauchfuss, V. Pelmenschikov, C. C. Pham, L. B. Gee, H. Wang, S. P. Cramer, *Inorg. Chem.* **2018**, *57*, 1988 – 2001.
[15] T. B. Liu, X. P. Wang, C. Hoffmann, D. L. DuBois, R. M. Bullock, *Angew. Chem. Int. Ed.* **2014**, *53*, 5300 – 5304; *Angew. Chem.* **2014**, *126*, 5404 – 5408.

Manuscript received: May 4, 2018
Accepted manuscript online: June 19, 2018
Version of record online: July 23, 2018

